A Compact Triple-Band Notched MIMO Antenna for UWB Systems

Ling Wu, Yingqing Xia, and Xia Cao

College of Physical Science and Technology, Huazhong Normal University
No. 152 Luoyu Road, Wuhan, Hubei 430070, People's Republic of China

Abstract ─ A miniaturization ultra-wideband (UWB) multiple-input-multiple-output (MIMO) antenna with triple-notched band function is presented in the paper. There are two similar monopole radiators in the UWB-MIMO system. Based on half-cutting method, the system only occupies 21×27 mm^2. Three inverted L-shaped slots are inserted to get three rejected bands for suppressing interference from 3.5 GHz WiMAX, 5.5 GHz WLAN, and 8.1 GHz X-band. With a T-shaped stub extruding from the ground plane, both impedance bandwidth and port isolation are effectively improved. The proposed antenna covers operating frequency band of 3.1-11 GHz except three notched bands, and has a low port isolation of better than -20 dB. Moreover, good radiation patterns, stable gain and low envelope correlation coefficient (ECC) also ensure that the designed antenna is helpful in UWB systems.

Index Terms ─ Half-cutting method, monopole antenna, multiple-input-multiple-output (MIMO), notched band, ultra-wideband (UWB).

I. INTRODUCTION

UWB technology has attracted heated discussion since FCC (Federal Communications Commission) permitted 3.1-10.6 GHz for UWB applications in 2002 [1]. Monopole antennas have many advantages of low profile, compact volume and easy manufacture and the like. However, there are some difficulties in antenna design, of which frequency interference is the main challenge. Some systems frequencies working in 3.1-10.6 GHz may severely affect UWB applications, like WiMAX (3.3-3.7 GHz), WLAN (5.15-5.825 GHz), and X-band (7.7-8.5 GHz). Design multiple band notched UWB antenna is a useful means to mitigate these interferences. The second challenge is multipath fading. As MIMO technology can significantly enhance the capacity of the system and resist multipath fading, it has become a hot spot in the field of wireless communication [2]. For above reasons, design UWB-MIMO antennas with multiple notched bands and low mutual coupling is promising.

In recent years, many reports about multiple notched bands for UWB systems have been discussed, such as inserting various structures (folded stepped-impedance resonators [3], CSRR structure [4], arc-shaped slots [5]). However these multiple notched-band antennas have a big size [3-5]. With half-cutting method [6,7], size of antenna can be reduced a lot. A LTCC antenna with compact size of 17×10 mm^2 was proposed [6]. And the dimension of antenna was decreased from 40×40 mm^2 to 10×20 mm^2 [7].

Recently, some technologies about improving port isolation of UWB-MIMO antennas have been reported [8-14]. [8] applied a tree-like decoupling element to get isolation of less than -16 dB. [9] adopted a sine-curve based nested T-shaped structure to obtain -20 dB port isolation. Neutralization lines were used in [10] to obtain isolation more than 22 dB. [11] introduced a rectangle stub as a decoupling structure to achieve -15 dB isolation. A T-shaped strip was placed between two radiators to alleviate mutual coupling [12]. Metal strips also can be applied to reduce isolation [13]. Without decoupling elements, two antennas were arranged vertically in [14] and high isolation of -20 dB was easily achieved.

Based on half-cutting method, a miniaturization triple band-notched UWB-MIMO antenna is introduced in the article. The whole size of the UWB-MIMO antenna is 21×27 mm^2 = 567 mm^2. Extruding a T-shaped stub on the back side, both impedance bandwidth and isolation are improved, which is the highlight of the design. Some decoupling elements in reports are just used to increase isolation, such as the decoupling structure in [8-12]. With inserting three inverted L-shaped slots on each radiator, triple notched bands are achieved for filtering 3.5 GHz WiMAX, 5.5 GHz WLAN, and 8.1 GHz X-band. Only one type of filter element with simple structure is adopted, so it is easy to adjust notched bands, which is another advantage of the design. Simple structure, triple-band notched characteristic and low mutual coupling make the antenna meaningful in UWB applications.

II. ANTENNA DESIGN

A. Configurations

The configuration of the UWB-MIMO antenna is exhibited in Fig. 1 (a). The system is etched on a 21×27×0.8 mm^3 FR4 substrate with dielectric constant

Submitted On: December 13, 2016
Accepted On: November 29, 2017

ε_r=4.4, loss tangent of 0.025. There are two identical monopole radiators in the system. Each radiator comprises a rectangular radiating patch with a beveled edge which is helpful for wider impedance bandwidth. A 50 ohm microstrip line of dimension Lf × wf is used for feeding each radiator. Three inverted L-shaped slots, labeled with Slot 1, Slot 2, Slot 3, are inserted in each radiator to mitigate 8.1 GHz X-band, 5.5 GHz WLAN and 3.5 GHz WiMAX separately. A T-shaped stub is extruded from the middle of the back ground, which is used to broaden impedance bandwidth and improve isolation.

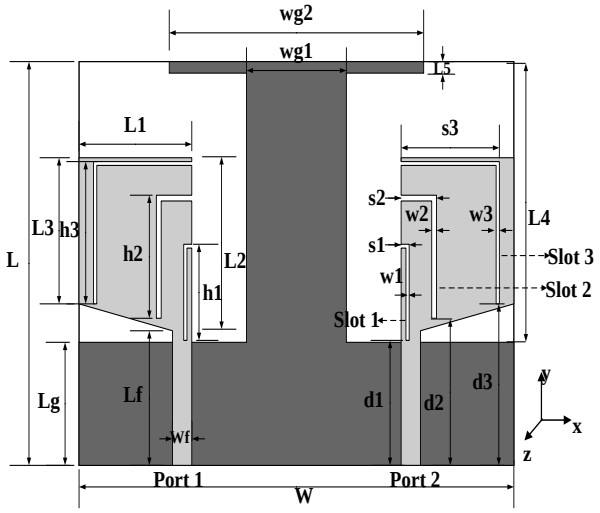

(a)

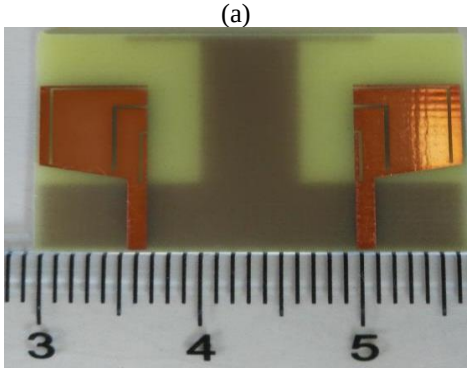

(b)

Fig. 1. (a) Schematic of proposed antenna, and (b) manufactured prototype.

In the design, total length of each inverted L-shaped slot is set to quarter of guided wavelength λ_g:

$$L = \frac{\lambda_g}{4} = \frac{c}{4f_c\sqrt{\varepsilon_{eff}}}, \quad (1)$$

where c denotes light speed, f_c is center frequency of corresponding notched band and,

$$\varepsilon_{eff} = \frac{(\varepsilon_r + 1)}{2} + \frac{(\varepsilon_r - 1)}{2}[1 + 12\frac{h}{W}]^{-1/2},$$

is effective dielectric constant.

Table 1 lists calculated L and simulated values. By comparison, the two are very close, which guarantees the design correctness.

Table 1: Calculated and simulated values

L	f_c (GHz)	Calculated Value (mm)	Simulated Value (mm)
L_1	3.5	11.1	13.3
L_2	5.5	7	8.3
L_3	8.1	4.8	5.3

CST Microwave Studio is applied in all simulations. The optimum parameters are obtained as follows (Unit: mm):

W=27, L=21, Lg=6.4, Lf=7, Wf=1.2, L1=7, L2=9, L3=7.6, L4=14, L5=0.6, wg1=6.2, wg2=15.8, s1=0.5, w1=0.2, h1=4.8, d1=6.5, s2=2.2, w2=0.3, h2=6.1, d2=7.65, s3=6.1, w3=0.2, h3=7.2, d3=8.4. As shown in Fig. 1 (b), a prototype was fabricated according to the above parameters.

B. Effect of the T-shaped stub

Figure 2 shows evolution of the ground plane. In the initial design, only a partial ground plane is applied, which is shown in Fig. 2 (a). In Fig. 2 (b), a T-shaped stub is added to the ground. The effects of the T shape ground on the antenna with and without those slots are shown in Fig. 3 and Fig. 4.

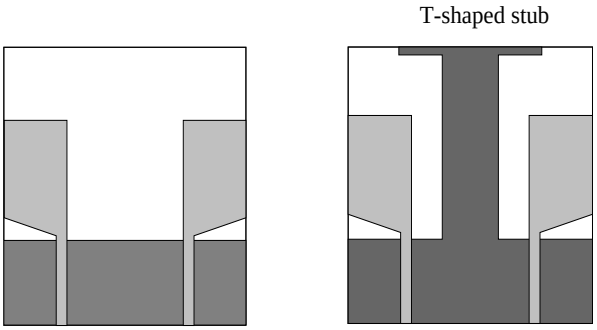

(a) Ant-1 (b) Ant-2

Fig. 2. Design evolution of the ground plane: (a) Ant-1 and (b) Ant-2.

Figure 3 plots S-parameters for the above antennas which named Ant-1, Ant-2, respectively. Due to symmetry of Port 1 and Port 2, only S11 and S21 are studied for simplicity. As plotted in Fig. 3 (a), without the T-shaped stub, the value of S11 is less than -10 dB from 5.5 to 11 GHz for Ant-1. For Ant-2, after adopting the T-shaped stub, a response is generated at 3.4 GHz. Thus, Ant-2 has a much lower frequency than Ant-1. And then the

proposed antenna can cover 3.1-11 GHz UWB band. In Fig. 3 (b), at low frequency band, the value of S21 is above -15 dB for Ant-1. However, it is less than -15 dB for Ant-2. So the T-shaped stub improves isolation.

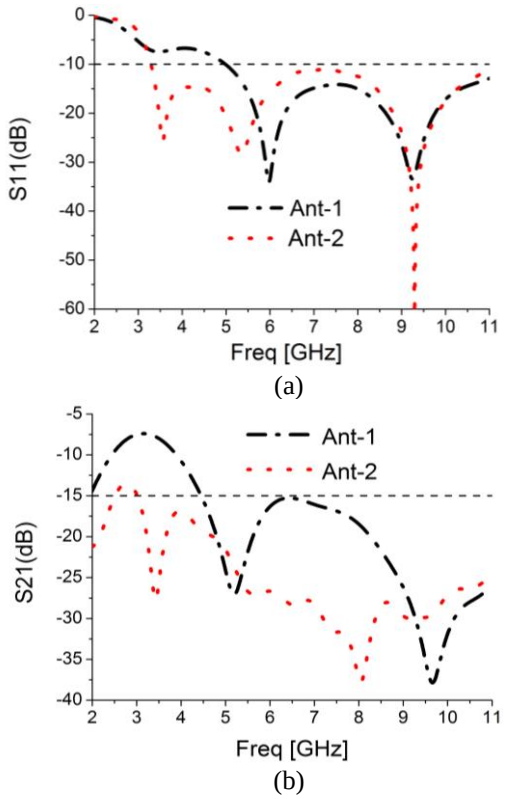

Fig. 3. (a) Simulated S11and (b) simulated S21.

Figure 4 shows surface current distributions at 4.5 GHz with/without the T-shaped stub and with/without three slots when Port1 is excited. From Fig. 4 (a), a lot of electric current is coupled to Port 2 without the stub. By contrast, with the stub, as shown in Fig. 4 (b), a large part of current is stopped from flowing to Port 2, and port isolation is greatly improved. The phenomenon of current tendency in Fig. 4 (c) is similar to Fig. 4 (a), and Fig. 4 (d) is similar to Fig. 4 (a). Whether or not there are slots on the patch, the T-shaped stub can reduce coupling. Figure 3 and Fig. 4 demonstrate that the T-shaped stub is not only used to broaden -10 dB impedance bandwidth, but also to reduce coupling.

C. Effects of inverted L-shaped slots (Slot 1, Slot 2, and Slot 3)

Figure 5 exhibits the effect of h3, h2, and h1 on S11, respectively. When one parameter is varied, the others are fixed. The effect of different h3 on S11 is plotted in Fig. 5 (a). When h3 grows from 7 to 7.4 mm, the length of Slot 3 becomes larger. The first notched band (denoted as NB) shifts slightly to the left, which can be deduced by formula (1). As Fig. 5 (b) shows, the second NB moves from 5.7 GHz to 5.3 GHz when the length of Slot 2 (h2) increases from 5.9 to 6.3 mm. In Fig. 5 (c), adjusting h1 from 4.6 mm to 5 mm, the length of Slot 1 is increased. Central frequency of the third NB is decreased from 8.5 GHz to 7.6 GHz. From Fig. 5, it also can be observed that when one NB was controlled, the other NBs keep almost unchanged. Thus, each NB can be adjusted individually.

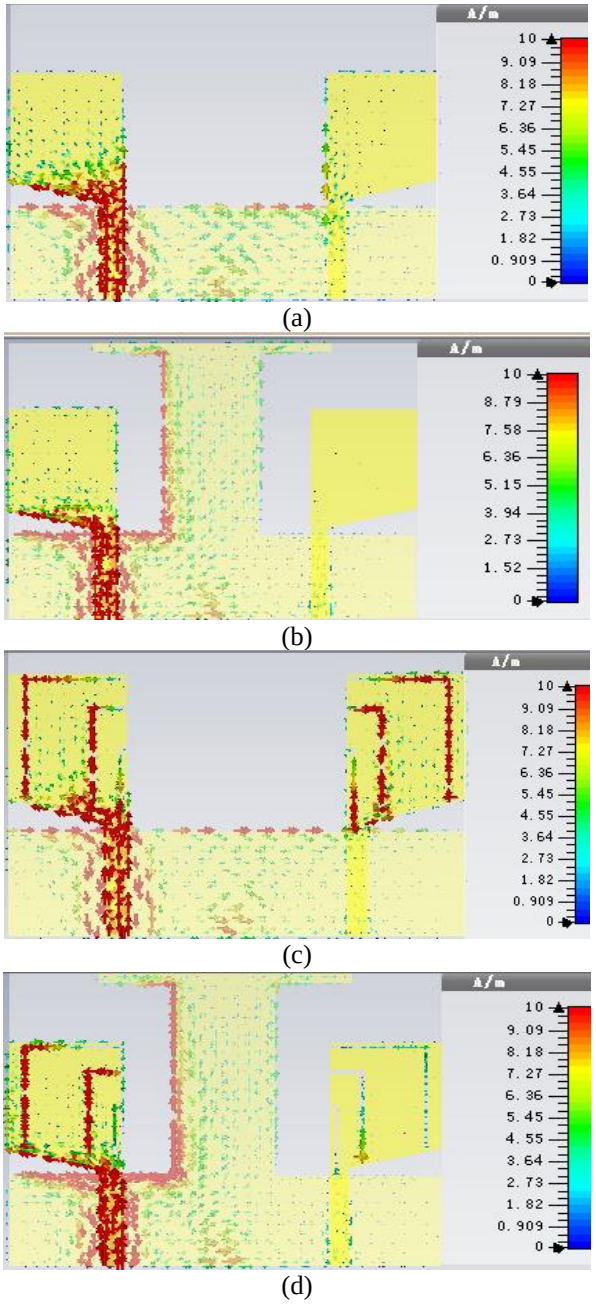

Fig. 4. Surface current distributions at 4.5 GHz: (a) without T-shaped stub, (b) with T-shaped stub, (c) with three slots and without T-shaped stub, and (d) with three slots and T-shaped stub.

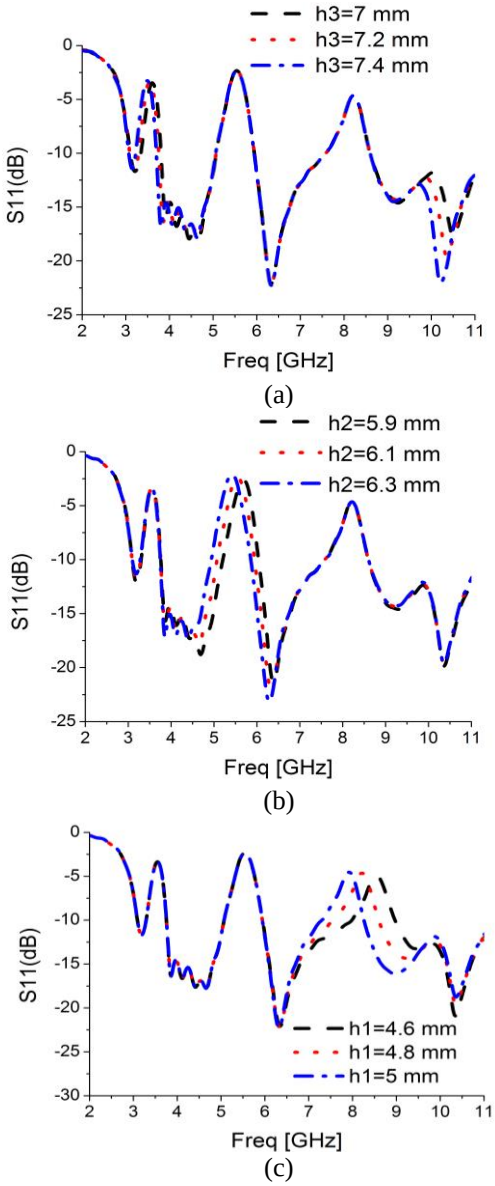

Fig. 5. Simulated S11: (a) effect of h3, (b) effect of h2, and (c) effect of h1.

Surface current distributions on the antenna at 3.5, 5.5, and 8.1 GHz are shown in Fig. 6, which help us to better understand the formation mechanism of rejected bands. From Fig. 6, at notched frequencies, strong electric current concentrates around the corresponding slot, which demonstrates that the slots play important role in the formation of NBs. Moreover, with the increase of the distance away from the feeding point, weaker current is appeared on the slots. At the top of the slots, weakest current and highest impedance is observed. These slots can be considered as a quarter-wavelength resonator, which converter nearly zero impedance to high impedance. The mismatch of impedance leads to the generation of NBs.

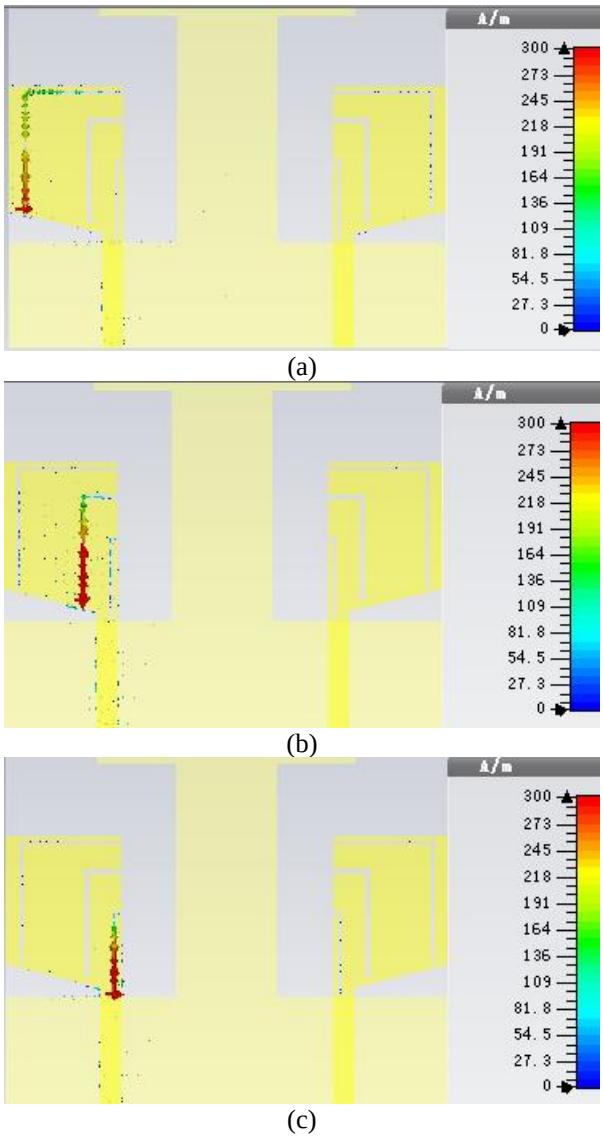

Fig. 6. Surface current distributions when Port 1 is excited: (a) 3.5 GHz, (b) 5.5 GHz, and (c) 8.1 GHz.

III. RESULTS AND DISCUSSIONS

To verify the introduced design method, the antenna was manufactured and tested. The S-parameters of the proposed antenna were measured with Agilent E8362B network analyzer. The results were gained when Port 1 was excited and Port 2 was terminated with a 50 ohm load. As shown in Fig. 7 (a), the introduced antenna maintains S11<-10 dB (or VSWR<2) from 3.1 to 11 GHz, except three notched bands of 3.3-3.75 GHz, 5.07-5.95 GHz and 7.6-8.6 GHz. That means the antenna can filter 3.5 GHz WiMAX, 5.5 GHz WLAN and 8.1 GHz X-band effectively. The same conclusion can be obtained in Fig. 7 (b). From Fig. 7 (c), the value of measured S21 is

smaller than -20 dB in the entire UWB band, which proves that the antenna can be used in MIMO applications. Measured results are in good accordance with simulated analysis except slight deviations, may be caused by manufacturing error and jointing of SMA connector.

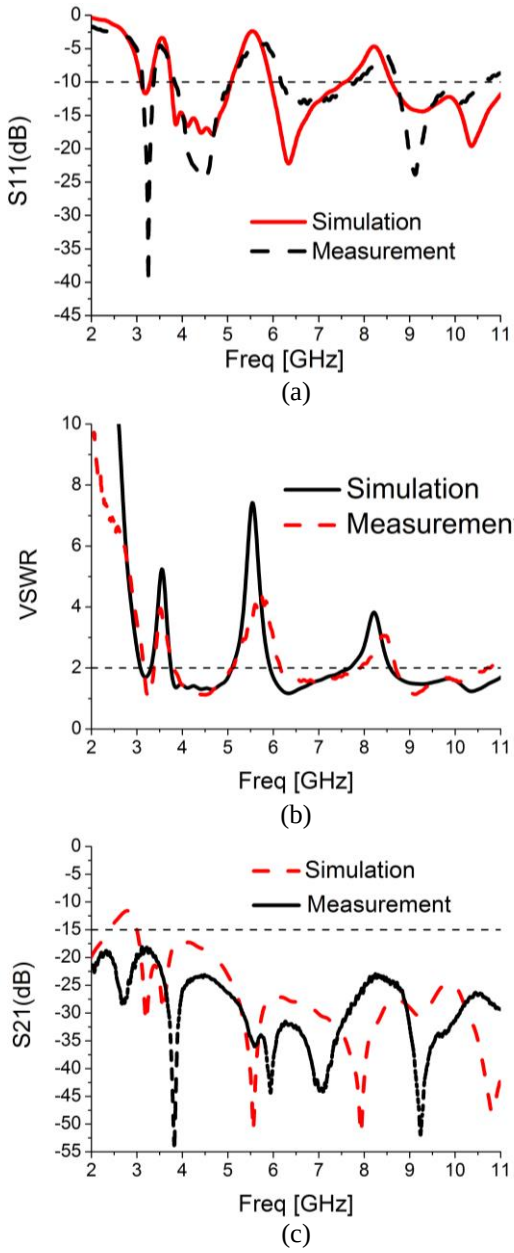

Fig. 7. Simulated and measured S-parameters of the proposed antenna: (a) S11, (b) VSWR, and (c) S21.

Figure 8 shows simulated normalized far field radiation patterns of y-z (E) plane and x-z (H) plane for Port 1 at 4, 6.5, and 9 GHz. It is similar to a dipole in y-z (E) plane, and quasi omnidirectional radiation pattern in the x-z (H) plane. Figure 9 (a) presents the comparison between the peak gain and the other azimuth angles when Port 1 is excited. From Fig. 9 (a), sharp drops are observed at 3.5 GHz, 5.5 GHz, and 8.1 GHz notched frequencies, while in the working band the peak gain is stable with less than 2 dB variation. In addition, when the azimuth angle is 60 degrees or 90 degrees, the gain is always less than the peak gain. Figure 9 (b) shows that radiation efficiency is above 70% except three lowest values at rejected bands.

In order to further evaluate MIMO diversity performance, ECC (envelope correlation coefficient) is analyzed. For two-port MIMO systems, ECC can be calculated by [15]:

$$\rho_e = \frac{\left|S_{11}^{*}S_{12} + S_{21}^{*}S_{22}\right|^2}{\left(1-\left|S_{11}\right|^2-\left|S_{21}\right|^2\right)\left(1-\left|S_{22}\right|^2-\left|S_{12}\right|^2\right)}, \quad (2)$$

for symmetry of Port 1 and Port 2, $S_{11}=S_{22}$, $S_{12}=S_{21}$. After obtaining measured S-parameters, ECC results are calculated by Eq. (2). Figure 10 shows that the ECC are below 0.04 across 3.1-10.6 GHz UWB band.

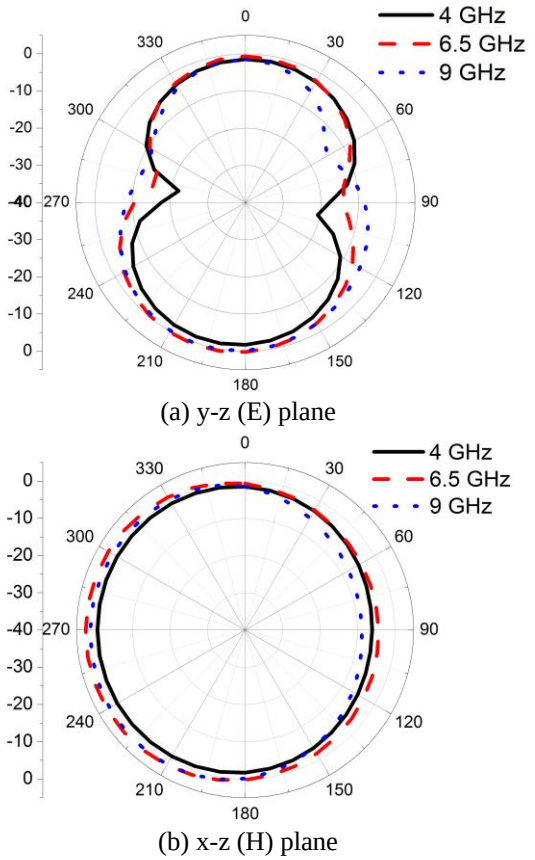

Fig. 8. Simulated normalized far field radiation patterns for Port 1.

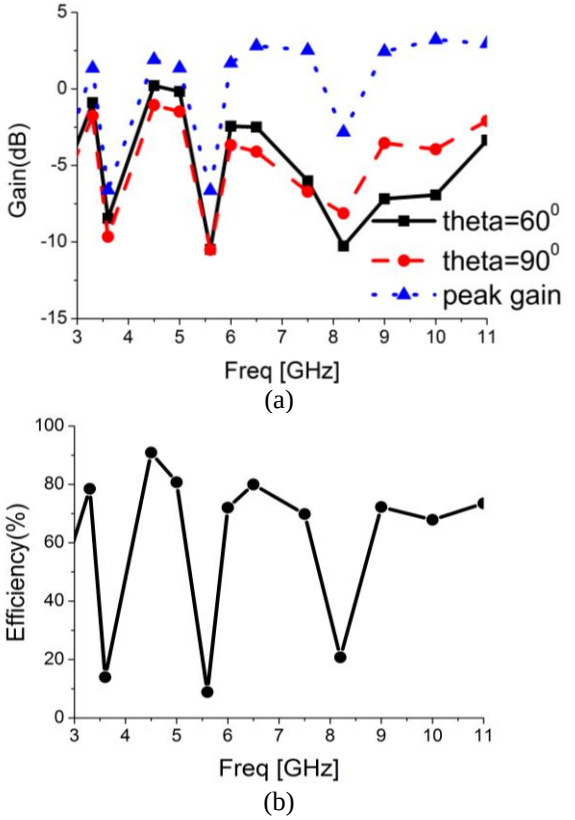

Fig. 9. (a) Simulated gain and (b) simulated radiation efficiency.

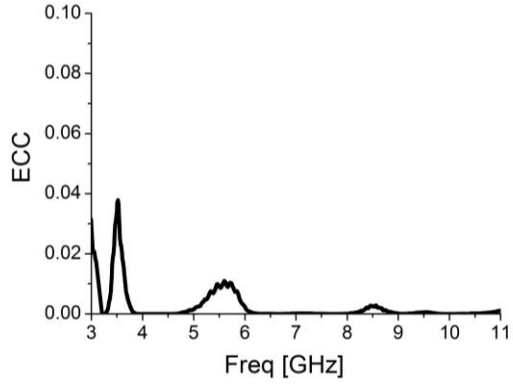

Fig. 10. Measured ECC of the proposed antenna.

Finally, Table 2 compares the introduced antenna with other UWB-MIMO systems. Antennas in [8,9] can cover UWB band, but without filtering performance. [10] introduces a novel decoupling structure (neutralization lines); however, 3.1-5 GHz band was covered. The antennas in [11,12] have 5.5 GHz notch function, but they are relatively large in size. With two notched band characteristic, the antenna in [13] has a bigger size and stronger mutual coupling than the proposed antenna. Also filtering for WiMAX, WLAN and X-band in [14], the proposed antenna has a smaller size. By comparison, this work has a more compact size, high isolation, and triple notched band characteristic.

Table 2: Comparisons of the introduced antenna and other UWB-MIMO antennas

Ref.	Size (mm^2)	Stop Bands (GHz)	Isolation (dB)	BW (GHz)
[8]	35×40	-	-16	3.1-10.6
[9]	30×50.5	-	-20	3.1-10.6
[10]	35×33	-	-22	3.1-5
[11]	48×48	5.5	-15	2.5-12
[12]	38.5×48.5	5.5	-15	3.08-11.8
[13]	30×40	3.5/5.5	-15	3.1-10.6
[14]	30×60	3.5/5.5/8	-20	2.8-11
This work	21×27	3.5/5.5/8.1	-20	3.1-11

*BW is bandwidth.

VI. CONCLUSION

With triple notched band function, a compact UWB-MIMO antenna has been designed and analyzed. Based on half-cutting method, the whole size is only 21×27 mm^2. Three inverted L-shaped slots are inserted on each radiator to notch 3.5 GHz WiMAX, 5.5 GHz WLAN and 8.1 GHz X-band. With a T-shaped stub extruding from the ground plane, the antenna can cover 3.1-11 GHz and high port isolation of -20 dB is achieved. Moreover, good radiation patterns, stable gain, and ECC of less than 0.04 prove it helpful in UWB applications.

ACKNOWLEDGMENT

The authors are grateful to the technical support of the Electromagnetic Laboratory in Huazhong Normal University.

REFERENCES

[1] FCC, “First report and order,” 2002. FCC: First report and order on ultra-wideband technology, Washington, DC, USA, 2002.

[2] T. Kaiser, Z. Feng, and E. Dimitrov, “An overview of ultra-wideband systems with MIMO,” *Proc. IEEE*, pp. 285-312, March 2009.

[3] T. Li, H. Q. Zhai, G. H. Li, L. Li, and C. H. Liang, “Planar ultrawideband antenna with multiple band-notches based on folded stepped-impedance resonator and defected split ring resonator,” *Microw. Opt. Technol. Lett.*, vol. 55, no. 3, pp. 600-603, March 2013.

[4] J. Y. Kim, N. Kim, S. Lee, and B. C. Oh, “Triple band-notched UWB monopole antenna with two resonator structures,” *Microw. Opt. Technol. Lett.*, vol. 55, no. 1, pp. 4-6, January 2013.

[5] J. Liu, K. P. Esselle, S. G. Hay, and S. S. Zhong, “Study of an extremely wideband monopole

antenna with triple band-notched characteristics," *Progress In Electromagnetics Research*, vol. 123, no. 8, pp. 143-158, January 2012.

[6] M. Sun, Y. P. Zhang, and Y. L. Lu, "Miniaturization of planar monopole antenna for ultra-wideband radios," *IEEE Trans. Antennas Propag.*, vol. 58, no. 7, pp. 2420-2425, August 2010.

[7] G. P. Gao, B. Hu, and J. S. Zhang, "Design of a miniaturization printed circular-slot UWB antenna by the half-cutting method,"*IEEE Antennas Wireless Propag. Lett.*, vol. 12, no. 1, pp. 567-570, December 2013.

[8] S. Zhang, Z. N. Ying, J. Xiong, and S. L. He, "Ultrawideband MIMO/diversity antennas with a tree-like structure to enhance wideband isolation," *IEEE Antennas Wireless Propag. Lett.*, vol. 8, no. 4, pp. 1279-1282, February 2009.

[9] M. Bilal, R. Saleem, M. F. Shafique, and H. A. Khan, "MIMO application UWB antenna doublet incorporating a sinusoidal decoupling structure," *Microw. Opt. Technol. Lett.*, vol. 56, no. 7, pp. 1547-1553, July 2014.

[10] S. Zhang and G. F. Pedersen, "Mutual coupling reduction for UWB MIMO antennas with a wideband neutralization line," *IEEE Antennas Wireless Propag. Lett.*, vol. 15, pp. 166-169, January 2016.

[11] P. Gao, S. He, and et al., "Compact printed UWB diversity slot antenna with 5.5-GHz band-notched characteristic," *IEEE Antennas Wireless Propag. Lett.*, vol. 13, no. 4, pp. 376-379, January 2014.

[12] L. Kang, H. Li, X. H. Wang, and X. W. Shi, "Compact offset microstrip-fed MIMO antenna for band-notched UWB applications," *IEEE Antennas Wireless Propag. Lett.*, vol. 14, pp. 1754-1757, January 2015.

[13] T. C.Tang and K. H. Lin, "An ultrawideband MIMO antenna with dual band-notched function," *IEEE Antennas Wireless Propag. Lett.*, vol. 13, pp. 1076-1079, January 2014.

[14] H. Huang, Y. Liu, S. S. Zhang, and S. X. Gong, "Compact polarization diversity ultrawideband MIMO antenna with triple band-notched characteristics," *Microw. Opt. Technol. Lett.*, vol. 57, no. 4, pp. 946-953, April 2015.

[15] S. Blanch, J. Romen, and I. Corbella, "Exact representation of antenna system diversity performance from input parameter description," *Electron. Lett.*, vol. 39, no. 9, pp. 705-707, June 2003.

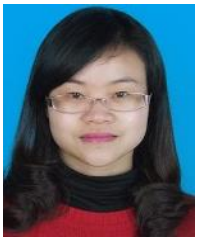

Ling Wu received M.S. degree in Huazhong Normal University in 2007. Currently, she is a Lecturer, and she is pursuing her Ph.D. Her main research includes microtrip-fed antenna design, signal processing.

Yingqing Xia received his Ph.D. in Huazhong Normal University in 2003. From 2006 to 2007, he engaged in postdoctoral research at the University of Oxford. Now he is a Professor who is interested in microwave circuits and hardware systems.